https://doi.org/10.17221/118/2019-SWR

Sponge effect of aerated concrete on phosphorus adsorption-desorption from agricultural drainage water in rainfall

*Jinquan Zhang, Weiguo Fu**

Key Laboratory of Modern Agricultural Equipment and Technology, Jiangsu University, Ministry of Education, Zhenjiang, P.R. China

**Corresponding author: fwguo168@sina.com*

Citation: Zhang J., Fu W. (2020): Sponge effect of aerated concrete on phosphorus adsorption-desorption from agricultural drainage water in rainfall. Soil & Water Res., 15: 220–227.

Abstract: In the initial stage of the rainfall, the nutrient element phosphorus (P) in the farmland, one of the most important factors causing agricultural non-point source pollution, flows into agriculture drainage ditches rapidly, and an instantaneous phosphorus peak value in the ditch water often occurs. Aerated concrete with high P adsorption properties was chosen as the experiment material in the laboratory to reduce the instantaneous P peak value in the drainage water in the initial stage of the rainfall. The three total P (TP) concentrations of the simulated drainage water (1.0, 2.0, and 3.0 mg/L) stood for three treatments were designed in the adsorption experiment; the same three TP concentrations of the simulated drainage water and the three TP concentrations of the simulated natural water (0.2, 0.3, and 0.4 mg/L) stood for nine treatments in the desorption experiment. The sponge effect of the aerated concrete on the P adsorption-desorption was explored by studying the dynamics of the P adsorption-desorption of the aerated concrete with an increase in the experiment's time. The results showed the following details: (1) Both the adsorption rate and desorption rate of the aerated concrete decrease with an increase in the experiment's time. The initial adsorption is dominant during the entire adsorption, as with the initial desorption during the entire desorption. (2) The adsorption capacity of the aerated concrete slightly decreases with the increase in the re-adsorption, whereas the desorption capacity of the aerated concrete significantly decreases with the increase in the re-desorption. Thus, the aerated concrete can be introduced into the agricultural drainage ditch to reduce the instantaneous P peak value in the drainage water in the initial stage of the rainfall, and potential further studies should explore the relationship between the different drainage water loads and the amount of the aerated concrete.

Keywords: aerated concrete; adsorption-desorption; agricultural drainage; sponge effect

In recent years, the problem of agricultural non-point source pollution has become increasingly prominent. This issue not only directly affects the water environment in the region, but also indirectly affects the ecological security of agricultural products. Research has shown that some nutrients in the farmland system are mainly lost through agricultural drainage systems (Williams et al. 2018). These lost nutrients are converted into a major component of agricultural non-point source pollution. An agricultural ecological ditch is a drainage treatment project through plant absorption, adsorption of a sediment or filler, and microbial degradation (Li et al. 2016; Wang et al. 2019). However, in the initial stage of the rainfall, the nutrient elements, such as nitrogen and phosphorus (P), in the farmland flow into the

Funding Supported by the National Natural Science Foundation of China [31370448], Postgraduate Research & Practice Innovation Program of Jiangsu Province [SJKY19_2528], and the Priority Academic Program Development of Jiangsu Higher Education Institutions [PAPD-2018-87].

https://doi.org/10.17221/118/2019-SWR

agriculture drainage ditches rapidly, and the instantaneous peak values of considerable pollution often arises in the ditch water. Studies have demonstrated that the pollution generated in the initial stage of the rainfall typically accounts for 50–80% of the total pollution generated during the entire rainfall (Lee et al. 2002; Kröger et al. 2008); consequently, agriculture drainage water frequently cannot meet the national discharge standards in the initial stage of the rainfall (Yang et al. 2016).

The constructed wetland system is another type of drainage treatment project. Its phosphorus removal mainly depends on the adsorption of fillers (Vohla et al. 2011). The amount of P removed using recycled brick as a filler often exceeds 80% of that of the entire project (Saeed et al. 2018). Fillers not only adsorb P from the drainage water with a high P concentration, but also desorb P into the water with a low P concentration after adsorbing a certain amount of P (Haddad et al. 2018). Aerated concrete, a common building material, is not only rich in Ca^{2+}, Al^{3+}, Fe^{3+}, Mg^{2+}, and other metal ions, but also contains numerous micro-voids, which facilitate its adsorption or desorption P (Zhang & Zhu 2018). Therefore, aerated concrete is widely used in sewage treatment. The theoretical maximum adsorption amount of aerated concrete reportedly reaches 6 064 mg/kg (Fu & Li 2011). Considering the adsorption-desorption characteristics of fillers, the possibility of using aerated concrete as a filler to reduce the instantaneous P peak value of the drainage water in the initial stage of rainfall was explored by studying the adsorption and desorption properties of the aerated concrete separately. That is, the aerated concrete initially adsorbs P from the agricultural drainage water with a high P concentration in the initial stage of the rainfall. With the continued rain, the P concentration of the ditch water gradually decreases, and a certain amount of P adsorbed in the initial stage of the rainfall is gradually desorbed from the aerated concrete into the ditch water with a low P concentration.

MATERIAL AND METHODS

Material. Aerated concrete was chosen as the experiment material. In practical applications, aerated concrete blocks are often cut into small pieces with various sizes to maximise its adsorption and desorption functions. In the present study, they were cut into small triangular prisms with a side length of 13.8 cm, a height of 10 cm, a mass of approximately 300 g, a bulk density of 0.36 g/cm^3, and a porosity of 74.2%, and their main components are shown in Table 1. The simulated agricultural drainage water and natural water with various P concentrations were prepared with potassium dihydrogen phosphate (KH_2PO_4). The simulated natural water was the lower P water used for the desorption experiments. HCl and NaOH were used to regulate the pH of the water to be 7 before the experiment.

P adsorption by aerated concrete. Studies have shown that the total P (TP) concentration in agricultural drainage water often reached 1–3 mg/L in the initial stage of rainfall (Liu 2016). Therefore, the TP concentrations of the simulated agricultural drainage water were set to 1.0, 2.0, and 3.0 mg/L in the adsorption experiment, representing three P concentration treatments of T_1, T_2, and T_3, respectively. In mid-May 2018, nine plastic barrels with the same specifications (20 cm in diameter and 22 cm in height) were selected, and a small piece of the abovementioned aerated concrete was placed in each barrel. Nine plastic barrels with a piece of aerated concrete were divided equally into three groups. Then, 3 L of the simulated drainage water with the TP concentrations of 1.0, 2.0, and 3.0 mg/L were poured into each barrel of the three groups, correspondingly. Therefore, the treatments with three replicates consisted of three P concentration levels of 1.0, 2.0, and 3.0 mg/L. Water samples of 10 ml were collected at 12, 24, 48, 72, 96, and 120 h after the start of the adsorption. The TP concentration of all the water samples were immediately determined by ammonium molybdate spectrophotometry (Chinese EPA 2002).

To explore the continuous adsorption capacity of the aerated concrete in multiple rainfalls, three 120 h continuous adsorption experiments were performed at the three P concentrations of the simulated drainage water for the abovementioned three treatments. That is, after the first 120 h adsorption experiment, the drainage water in each barrel was replaced with the newly configured drainage water with the same

Table 1. The main components of the aerated concrete

Components	SiO_2	CaO	Al_2O_3	Fe_2O_3	MgO	K_2O	Na_2O	Other components
Percentage of mass (%)	42.87	28.48	6.68	2.39	1.73	1.08	0.48	16.29

https://doi.org/10.17221/118/2019-SWR

volume and concentration. Subsequently, the water samples were collected at 12, 24, 48, 72, 96, and 120 h after the start of the re-adsorption. After the second 120 h adsorption experiment, a third 120 h adsorption experiment was similarly performed. The P adsorption amount of the aerated concrete (Q_a, mg/kg) is calculated as

$$Q_a = (C_0 - Ce)V/M$$

where:

C_0 – the initial TP concentration of the drainage water for the adsorption experiment (mg/L),

Ce – the TP concentration of the drainage water at each measurement time point during the adsorption (mg/L),

V – the volume of the drainage water in each barrel (L),

M – the mass of the piece of aerated concrete (g).

P desorption from aerated concrete. In mid-May 2018, 27 pieces of aerated concrete were divided equally into 3 groups. Each piece of the aerated concrete in the three groups was placed in 20 L of the simulated drainage water with the TP concentrations of 1.0 mg/L (T_a), 2.0 mg/L (T_b), and 3.0 mg/L (T_c), correspondingly. After 30 days of adsorption, the aerated concrete was taken out and air-dried for 7 days and then was used in the P desorption experiment.

In accordance with the China Environmental Quality Standards for Surface Water (GB 3838-2002), the TP concentrations of the simulated low P natural water were set to 0.2 (T_A), 0.3 (T_B), and 0.4 (T_C) mg/L in the desorption experiment. A total of 27 plastic barrels with uniform specifications (30.0 cm in diameter and 32.5 cm in height) were selected and divided equally into nine groups representing nine treatments (Table 2). Therefore, the treatments with three replicates were called T_{aA}, T_{aB}, T_{aC}, T_{bA}, T_{bB}, T_{bC}, T_{cA}, T_{cB}, and T_{cC}. A piece of the aerated concrete and the corresponding TP concentration of 10 L of the simulated natural water were placed into each barrel. Water samples of 10 ml were collected at 2, 4, 8, 12, 24, and 48 h after the start of the desorption.

Three continuous 48 h desorption experiments were performed in the three P concentrations of the simulated natural water to explore the continuous desorption capacity of the aerated concrete. That is, after the first 48 h desorption experiment, the natural water in each barrel was replaced with the newly configured natural water with the same volume and concentration. Then, the water samples were collected at 2, 4, 8, 12, 24, and 48 h after the start of the re-desorption. After the second 48 h desorption experiment, a third 48 h desorption experiment was similarly conducted (Chinese EPA 2002). The P desorption amount of the aerated concrete (Q_d, mg/kg) is calculated as

$$Q_d = (Ce'-C_0')V'/M'$$

where:

C_0' – the initial TP concentration of the natural water for the desorption experiment (mg/L),

Ce' – the TP concentration of the natural water at each measurement time point during the desorption (mg/L),

V' – the volume of the natural water used in each barrel (L),

M' – the mass of the piece of aerated concrete (g).

Statistical analysis. To test the differences among the treatments by SPSS 21, the data was analysed using an analysis of variance (ANOVA). The means were compared with the least significant difference test at a 5% level (George & Mallery 2013).

RESULTS AND DISCUSSION

P adsorption dynamics of the aerated concrete. The P adsorption dynamics of the aerated concrete in the T_1, T_2, and T_3 (Figure 1) treatments showed that the amount of P adsorption increases with the water P concentration with a coefficient of correlation of 0.8294. The total adsorption amounts during the 120-h adsorption treatment were 9.37, 18.82, and 28.45 mg/kg in T_1, T_2, and T_3, respectively. Significant differences were observed in the accumulative adsorption amounts

Table 2. The experimental treatments for the phosphorus desorption by the aerated concrete

Treatments of different concentrations		TP concentrations of water for desorption (mg/L)		
		T_A (0.2)	T_B (0.3)	T_C (0.4)
TP concentrations of water for adsorption (mg/L)	T_a (1.0)	TaA	TaB	TaC
	T_b (2.0)	TbA	TbB	TbC
	T_c (3.0)	TcA	TcB	TcC

TP – total phosphorus

https://doi.org/10.17221/118/2019-SWR

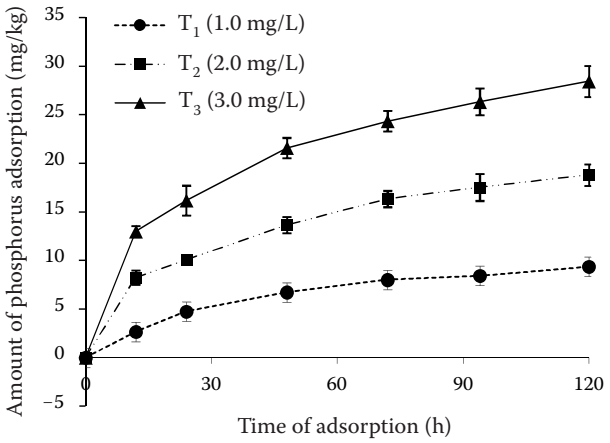

Figure 1. The phosphorus adsorption dynamics of the aerated concrete under the different treatments

among the three treatments at each measurement time point during the entire adsorption. The increase in the adsorption capacity with the water P concentration enabled the aerated concrete to adsorb the additional P easily from the agricultural drainage water in the initial stage of the rainfall.

During the 120-h adsorption treatment, the amount of P adsorption by the aerated concrete in the initial stage of the rainfall increased sharply and then slowly. The adsorption amount noted during first 12 h from the total adsorption amount during the 120 h were 28.38, 43.85, and 45.72% in T_1, T_2, and T_3, respectively. Afterward, during first 24 h adsorption accounted for 50.78, 53.53, and 56.91% in T_1, T_2, and T_3, respectively. The dominance of the initial absorption of the aerated concrete during the entire adsorption resulted in the effective adsorption of P from the agricultural drainage water in the initial stage of the rainfall.

Continuous adsorption capacity of the aerated concrete. In the simulated drainage water, the total amount of the P adsorption by the aerated concrete in each of the three 120 h continuous adsorption stages is shown in Table 3. The total adsorption amount in each adsorption stage gradually decreased with the continued adsorption. In comparison with the total adsorption amounts in the first stage, those in the second and third stages decreased slightly in the water with the different TP concentrations. The statistical analysis showed no significant differences in the total adsorption amounts among the three adsorption stages in the water with the same P concentration. These results indicated that the adsorption capacities of the aerated concrete in the three adsorption stages decrease constantly with the continued adsorption, but the decline is small. This phenomenon showed that the aerated concrete can still retain a high P adsorption capacity in multiple rainfalls.

Considering the important role of the initial adsorption during the entire adsorption, the percentages of the adsorption amount during the first 12 h of adsorption to the total adsorption amount during the 120-h adsorption treatment in the three continuous adsorption stages were provided (Table 4). The

Table 3. The total amounts of the phosphorus adsorption by the aerated concrete under the different adsorption conditions (mg/kg)

Three 120 h continuous adsorption stages	TP concentrations of water for adsorption (mg/L)		
	1.0	2.0	3.0
1st stage	9.37 ± 0.03[a]	18.82 ± 0.11[b]	28.45 ± 0.20[c]
2nd stage	8.86 ± 0.37[a]	18.28 ± 0.40[b]	27.90 ± 0.28[c]
3rd stage	8.87 ± 0.36[a]	18.09 ± 0.30[b]	27.83 ± 0.30[c]

TP – total phosphorus; the means within a column followed by the same letter are not significantly different at the level of 5%

Table 4. The percentages of the accumulative adsorption amount during the first 12 h of adsorption to the total adsorption amount during the 120-h adsorption (%)

Three 120 h continuous adsorption stages	TP concentrations of water for adsorption (mg/L)		
	1.0	2.0	3.0
1st stage	28.38 ± 4.21[a]	43.85 ± 3.92[b]	45.72 ± 1.64[c]
2nd stage	26.10 ± 4.27[a]	42.49 ± 0.88[b]	45.33 ± 1.64[c]
3rd stage	23.72 ± 2.25[a]	41.68 ± 2.47[b]	43.46 ± 0.83[c]

TP – total phosphorus; the means within a column followed by the same letter are not significantly different at the 5% level

https://doi.org/10.17221/118/2019-SWR

percentages in the water with the different P concentrations gradually decreased with the continued adsorption, but the declines are small. No significant differences in the percentage were observed between any two adsorption stages in the water with the same P concentration, thereby indicating that the dominance of the initial absorption of the aerated concrete was maintained well in the multiple rainfalls.

The P adsorption capacity of the filler can be affected by various factors, such as the P concentration and the pH of the water, the particle size of the filler, the adsorption time, and other environmental factors (Özacar 2003; Mor et al. 2016; Hou et al. 2018). The results showed that the P concentration in the water significantly affects the P adsorption capacity of the aerated concrete. This finding is consistent with those of previous studies (Deng & Wheatley 2018; Zhang & Zhu 2018; Castellar et al. 2019). Cucarella and Renman (2009) emphasised that high solute concentrations encourage other adsorption mechanisms, such as substantial boundary concentrations; Zhang highlighted that the P adsorption of a filler is only attributed to the physical adsorption in low P concentration water, while the high P concentration of the water can sufficiently cause chemical reactions, such as complexation and precipitation, with the metals (Zhang et al. 2005). In addition, some works have reported that the equilibrium adsorption capacity of aerated concrete for phosphorus reaches 300–6064 mg/kg, which is much higher than the amount of the P adsorption obtained in the present study (Fu & Li 2011; Deng & Wheatley 2018; Zhang & Zhu 2018; Castellar et al. 2019). The results of the above studies were mainly due to them being based on kinetic bath studies of aerated concrete, which was crushed into a powder and then placed in extremely high P concentration water (5–60 mg/L), and the gained equilibrium adsorption capacity was nearly the theoretical maximum. However, in the present study, the aerated concrete blocks were initially cut into the abovementioned small triangular prisms, while the TP concentration of the simulated drainage water was only 1.0–3.0 mg/L.

P desorption dynamics of the aerated concrete. The P desorption dynamics of the aerated concrete under the different treatments are illustrated in Figure 2. In the nine treatments, the desorption amount of the aerated concrete with a pre-adsorption amount of 198.80 mg/kg (i.e., T_{cA}, T_{cB}, and T_{cC}) continuously increased during the 48 h desorption, and the desorption amount during the initial 12 h desorption accounted for approximately 55.83–59.78% of the total desorption amount within the 48 h desorption. Those of the aerated concrete with the pre-adsorption amounts of 28.51 and 105.13 mg/kg (i.e., T_{aA}, T_{aB}, T_{aC}, T_{bA}, T_{bB}, and T_{bC}) constantly increased to the maximum during the first 12 h initial desorption, but then fluctuated slightly, indicating that the desorption and adsorption

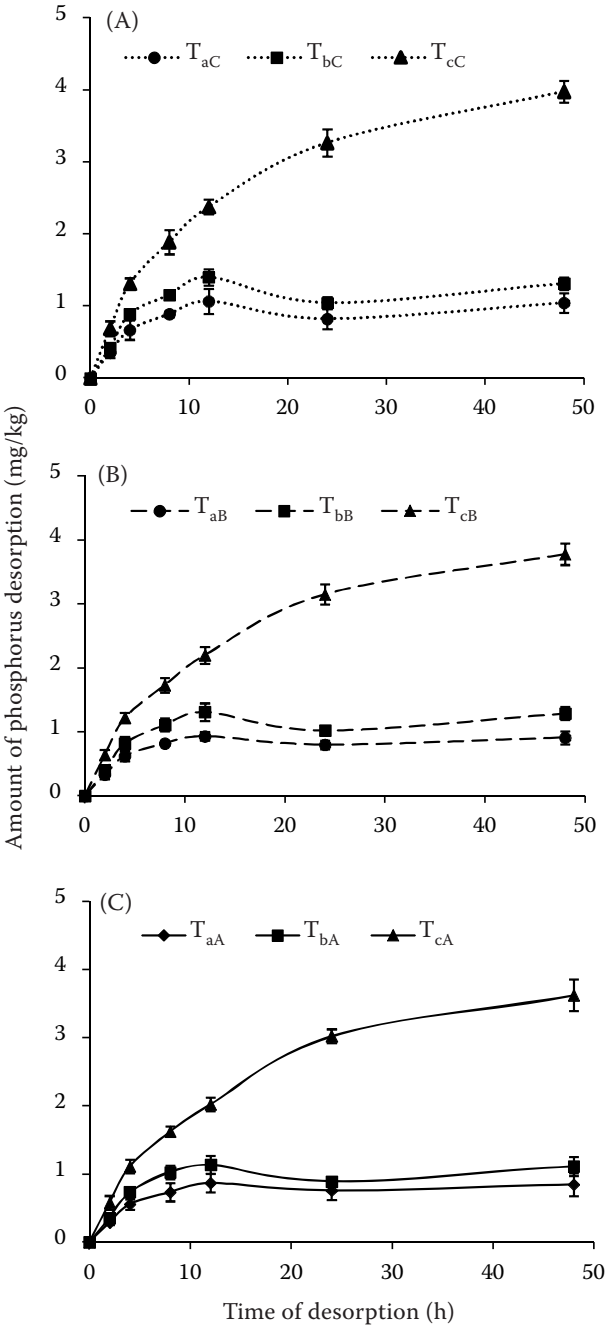

Figure 2. The phosphorus desorption dynamics of the aerated concrete under the different treatments: 0.2 mg/L (A), 0.3 mg/L (B), 0.4 mg/L (C)

https://doi.org/10.17221/118/2019-SWR

Table 5. The total desorption amount from the aerated concrete during the 48-h desorption under the different treatments (mg/kg)

Treatments of different concentrations		TP concentrations of water for desorption (mg/L)		
		T_A (0.2)	T_B (0.3)	T_C (0.4)
TP concentrations of water for adsorption (mg/L)	T_a (1.0)	α 1.04 ± 0.14^c	α 0.91 ± 0.10^c	α 0.84 ± 0.17^c
	T_b (2.0)	β 1.31 ± 0.08^b	β 1.29 ± 0.10^b	β 1.11 ± 0.14^b
	T_c (3.0)	γ 3.98 ± 0.10^a	γ 3.78 ± 0.17^a	γ 3.62 ± 0.23^a

TP – total phosphorus; the means with the same letter before it within a line are not significantly different at the 5% level; the means within a column followed by the same letter are not significantly different at the 5% level

occurred simultaneously after the first 12 h initial desorption. Therefore, the initial 12 h desorption was dominant during the entire desorption.

The total desorption amounts of the aerated concrete during the 48-h desorption in the nine treatments are provided in Table 5. In the same P concentrations of the water for the desorption (i.e., T_A, T_B, or T_C), the total desorption amount of the aerated concrete significantly increased with the P concentration of the water, and significant differences in the total desorption amounts were observed among the three P concentrations of the water (i.e., T_a, T_b, and T_c). For the aerated concrete in the same P concentration of the water for the adsorption (i.e., T_a, T_b, or T_c), the total desorption amount gradually decreased with the increase in the P concentration of the water. However, no significant differences in the total desorption amount were observed among the three P concentrations of the water for the desorption (i.e., T_A, T_B, and T_C).

Continuous desorption capacity of the aerated concrete. Table 6 showed that the total desorption amount from the aerated concrete in each of three desorption stages gradually decreased, and the declines increased with the P concentrations of the natural water. Significant differences in the total desorption amounts were observed between any two of the three stages. Among the three TP concentrations of the water for adsorption, the highest total desorption percentages were observed in the adsorption water with a TP concentration of 1.0 mg/L, regardless of the TP concentrations of the water for the desorption. This result is consistent with other findings in which adsorption is only attributed to the physical adsorption in the lower concentrations of the water, thereby enabling an easy P release (Zhang et al. 2005; Deng & Wheatley 2018; Zhang & Zhu 2018).

Numerous studies on P desorption from fillers have been conducted, but most of those studies have primarily focused on the secondary pollution due to the P desorption from the fillers (Paradelo et al. 2016; Li et al. 2017; Zhou et al. 2019). However, that a certain amount of P desorption from the fillers into the low P concentration water urges the aerated concrete to empty part of P adsorption capacity, and then the aerated concrete can re-adsorb the P well when the high P concentration water appears again in the next rainfall. In the present study, the mean of the total desorption percentage was 5.00%. This finding is basically consistent with the results of other studies in which the P desorption percentage from aerated concrete in deionised water is 4–7% (Deng & Wheatley 2018). The P desorption percentage from the aerated concrete

Table 6. The total desorption capacity of the aerated concrete in the three 48 h continuous desorption stages (mg/kg)

Three 48 h continuous desorption stages	TP concentration of water for adsorption (mg/L)								
	1.0			2.0			3.0		
	TP concentrations of water for desorption (mg/L)								
	0.2	0.3	0.4	0.2	0.3	0.4	0.2	0.3	0.4
1st stage	1.04 ± 0.14^a	0.91 ± 0.10^a	0.84 ± 0.17^a	1.31 ± 0.08^a	1.29 ± 0.10^a	1.11 ± 0.14^a	3.98 ± 0.10^a	3.78 ± 0.17^a	3.62 ± 0.23^a
2nd stage	0.82 ± 0.04^b	0.69 ± 0.04^b	0.58 ± 0.04^b	1.13 ± 0.07^b	1.09 ± 0.04^b	0.89 ± 0.04^b	3.56 ± 0.10^b	3.20 ± 0.07^b	2.96 ± 0.27^b
3rd stage	0.56 ± 0.04^c	0.40 ± 0.07^c	0.32 ± 0.07^c	0.91 ± 0.04^c	0.82 ± 0.04^c	0.60 ± 0.07^c	3.11 ± 0.08^c	2.58 ± 0.14^c	2.33 ± 0.12^c
Total desorption percentage (%)	8.49	7.01	6.10	3.19	3.04	2.47	5.36	4.81	4.48

TP – total phosphorus; the means within a column followed by the same letter are not significantly different at the 5% level

https://doi.org/10.17221/118/2019-SWR

should be much higher in an agricultural drainage ditch than in the abovementioned experiments. This result was due to the volume of the simulated natural water for the desorption in the experiments is limited, and the small amount of P that was desorbed into the water will weaken the further desorption capacity of the aerated concrete during the desorption. Moreover, in relative terms, the volume of the water in the agricultural drainage ditch was nearly infinite, and large amounts of P that desorbed into the water would not reduce the further desorption capacity of the aerated concrete during the desorption.

CONCLUSION

An evident P absorption by the aerated concrete was observed in the high P concentration water, whereas the apparent P desorption from the aerated concrete was observed in the low P concentration water. The amounts of adsorption and desorption of the aerated concrete were highly positively and negatively related to the P concentration in the water, respectively.

Both the adsorption rate and desorption rate of the aerated concrete decrease with an increase in the experiment's time. The initial adsorption is dominant during the entire adsorption, as with the initial desorption during the entire desorption.

In the three continuous adsorption experiments, the adsorption capacity of the aerated concrete slightly decreased with the increase in the re-adsorption, but no significant difference among the three continuous 120 h adsorption treatments was observed. In the three continuous 48 h desorption treatments, the desorption capacity of the aerated concrete gradually decreased with the increase in the re-desorption, and a significant difference was observed among the three continuous 48 h desorption treatments.

Thus, the sponge effect of the aerated concrete on the P adsorption–desorption is evident, and it can be introduced into agricultural drainage ditches to reduce the instantaneous phosphorus peak value in the drainage water in the initial stage of the rainfall. Potential further studies will explore the relationship between the different drainage water load and the amount of the aerated concrete.

REFERENCES

Castellar J.A.D.C., Formosa J., Chimeno J.M., Canals J., Bosch M., Rosell J.R., Silva H.P.D., Morató J., Brix H., Arias C.A. (2019): Crushed Autoclaved Aerated Concrete (CAAC), a potential reactive filter medium for enhancing phosphorus removal in nature-based solutions – preliminary batch studies. Water, 11: 1442.

Chinese EPA (2002): Methods for Water and Wastewater Analysis. Vol. 3, 4th Ed. Beijing, Environmental Science Publishing House of China, 246–248. (in Chinese)

Cucarella V., Renman G. (2009): Phosphorus sorption capacity of filter materials used for on-site wastewater treatment determined in batch experiments – a comparative study. Journal of Environmental Quality, 38: 381–392.

Deng Y., Wheatley A. (2018): Mechanisms of phosphorus removal by recycled crushed concrete. International Journal of Environmental Research and Public Health, 15: 357.

Fu W.G., Li P.P. (2011): Characteristics of phosphorus adsorption of aerated concrete in wastewater treatment. Advanced Materials Research, 183–185: 466–470.

George D., Mallery P. (2013): IBM SPSS Statistics 21 Step by Step: A Simple Guide and Reference.Vol.12, Boston, Pearson Education: 164–172.

Haddad K., Jellali S., Jeguirim M., Trabelsi H.A.B., Limousy L. (2018): Investigations on phosphorus recovery from aqueous solutions by biochars derived from magnesium-pretreated cypress sawdust. Journal of Environmental Management, 216: 305–314.

Hou Q.J., Meng P.P., Pei H.Y., Hu W.R., Chen Y. (2018): Phosphorus adsorption characteristics of alum sludge: Adsorption capacity and the forms of phosphorus retained in alum sludge. Materials Letters, 229: 31–35.

Kröger R., Holland M.M., Moore M.T., Cooper C.M. (2008): Agricultural drainage ditches mitigate phosphorus loads as a function of hydrological variability. Journal of Environmental Quality, 37: 107–113.

Lee J.H., Bang K.W., Ketchum L.H., Choe J.S., Yu M.J. (2002): First flush analysis of urban storm runoff. Science of the Total Environment, 293: 163–175.

Li S.M., Wang X.L., Tu J.M., Qiao B., Li J.S. (2016): Nitrogen removal in an ecological ditch based on an orthogonal test. Water, Air, & Soil Pollution, 227: 396.

Li S.Y., Cooke R.A., Wang L., Ma F., Bhattarai R. (2017): Characterization of fly ash ceramic pellet for phosphorus removal. Journal of Environmental Management, 189: 67–74.

Liu D. (2016): Research on efficient collection technology of agricultural sewage on the east basin of Dianchi [MA.Eng. Thesis.] Chongqing, Chongqing University. (in Chinese)

Mor S., Chhoden K., Ravindra K. (2016): Application of agro-waste rice husk ash for the removal of phosphate from the wastewater. Journal of Cleaner Production, 129: 673–680.

Özacar M. (2003): Adsorption of phosphate from aqueous solution onto alunite. Chemosphere, 51: 321–327.

https://doi.org/10.17221/118/2019-SWR

Paradelo R., Conde-Cid M., Cutillas-Barreiro L., Arias-Estéveza M., Nóvoa-Muñoza J.C., Álvarez-Rodríguezb E., Fernández-Sanjurjob M.J., Núñez-Delgadob A. (2016): Phosphorus removal from wastewater using mussel shell: Investigation on retention mechanisms. Ecological Engineering, 97: 558–566.

Saeed T., Muntaha S., Rashid M., Sun G.Z., Hasnat A. (2018): Industrial wastewater treatment in constructed wetlands packed with construction materials and agricultural by-products. Journal of Cleaner Production, 189: 442–453.

Vohla C., Kõiv M., Bavor H.J., Chazarenc F., Mander Ü. (2011): Filter materials for phosphorus removal from wastewater in treatment wetlands: A review. Ecological Engineering, 37: 70–89.

Wang J.L., Chen G.F., Zou G.Y., Song X.F., Liu F.X. (2019): Comparative on plant stoichiometry response to agricultural non-point source pollution in different types of ecological ditches. Environmental Science and Pollution Research, 26: 647–658.

Williams M.R., Livingston S.J., Penn C.J., Smith D.R., King K.W., Huang C.H. (2018): Controls of event-based nutrient transport within nested headwater agricultural watersheds of the western Lake Erie basin. Journal of Hydrology, 559: 749–761.

Yang F., Jiang Y.F., Wang C.C., Huang X.N., Wu Z.Y., Chen L. (2016): Characteristics of nitrogen and phosphorus losses in Longhong Ravine Basin of Westlake in rainstorm. Environmental Science, 37: 141–147. (in Chinese)

Zhang X.L., Zhu G.C. (2018): Effect and mechanism of phosphorus adsorption in initial rainfall runoff by autoclaved aerated concrete block. Chinese Journal of Environmental Engineering, 12: 2202–2209. (in Chinese)

Zhang Y., Zou Y., Huang Y., Wang C., Li F. (2005): Phosphate adsorption and desorption characteristic of several fly ashes. Chinese Journal of Applied Ecology, 16: 1756–1760. (in Chinese)

Zhou H.X., Bhattarai R., Li Y.K., Li S.Y., Fan Y.H. (2019): Utilization of coal fly and bottom ash pellet for phosphorus adsorption: Sustainable management and evaluation. Resources, Conservation and Recycling, 149: 372–380.

Received: September 16, 2019
Accepted: March 16, 2020
Published online: April 8, 2020